TUDelft

Delft University of Technology

Risk-averse Estimation of Electric Heat Pump Power Consumption

Damianakis, Nikolaos; Mouli, Gautham Chandra Ram; Bauer, Pavol

Citation (APA)
Damianakis, N., Mouli, G. C. R., & Bauer, P. (2023). Risk-averse Estimation of Electric Heat Pump Power Consumption. In *CPE-POWERENG 2023 - 17th IEEE International Conference on Compatibility, Power Electronics and Power Engineering* (CPE-POWERENG 2023 - 17th IEEE International Conference on Compatibility, Power Electronics and Power Engineering). IEEE. https://doi.org/10.1109/CPE-POWERENG58103.2023.10227424

Important note
To cite this publication, please use the final published version (if applicable).
Please check the document version above.

Risk-averse Estimation of Electric Heat Pump Power Consumption

1st Nikolaos Damianakis
Electrical Sustainable Energy
Delft University of Technology
Delft, Netherlands
N.Damianakis@tudelft.nl

2nd Gautham Chandra Ram Mouli
Electrical Sustainable Energy
Delft University of Technolog
Delft, Netherlands
G.R.ChandraMouli@tudelft.nl

3rd Pavol Bauer
Electrical Sustainable Energy
Delft University of Technology
Delft, Netherlands
P.Bauer@tudelft.nl

Abstract—An important aspect of the energy transition is the expected grid impact due to the abrupt increase of distributed electric generation and electric load demand. A part of this impact is going to be inflicted by the electrification of heating with heat pumps (HPs). Therefore, it is essential that the future power consumption of electric heating is estimated. This work develops a power estimation model without the use of heating demand data, needing only weather data and building & heat pump specifications. Moreover, it is characterized as a risk-averse estimation since it uses no optimal control and utilizes the heat pump output capacity curves giving simultaneous priority to the customers' thermal comfort. Finally, it also estimates the power savings of electric heating due to future buildings' new insulation and energy label norms, revealing their importance.

Index Terms—air-sourced heat pumps, power consumption, insulation, COP, floor-heating

I. INTRODUCTION

The residential and services sectors produce a high amount of carbon emissions. Heating alone is also an important contributor to environmental pollution since in Europe, heating is mainly produced by gas-fired boilers [1]. An analysis of the EU-27 showed that in 2010, 24-26.7% of the annual fossil fuel-based energy was used by the residential sector alone. In the Netherlands, buildings account for 28% of the final demand consumption and 28% of natural gas consumption for heating [2]. Therefore, heating electrification by heat pumps (HPs) is of high importance to the energy transition. However, the quantification of the future HP power consumption and, consequently, the grid impact produced by heating electrification is essential to deal with the potential future hazards, e.g. power peaks, voltage deviations, and over-loading.

II. LITERATURE REVIEW

A lot of works have already focused on modeling the heating of a building by an HP. White-box detailed models of buildings and HP operation can be found in [3] & [4] and [5], respectively. While these works provide high accuracy and consider important details of the models, they are usually computationally expensive and unsuitable for grid-level studies comprising thousands of buildings. In contrast with the black-box models, which provide no knowledge about the governing laws of HP operation, grey-box models can provide an efficient trade-off between accuracy and computational burden. Such

heating models of buildings with HPs can be found in [6], [7], and [8]. While in [7], the impact of various water flow rates has been investigated, [6] focused on analyzing the effect of variable PV installation sizes and electricity prices. However, these three works model a Building Energy Management System (BEMS) and use a buffer tank for both space and water heating. Moreover, their models depend on the availability of a lot of information, such as heating demand data. In this work, an HP power consumption estimator has been developed, which uses no optimality with the aim of providing risk-averse HP power consumption profiles appropriate for grid studies. Moreover, the estimator depends only on very few easily accessible data, such as basic HP & building specifications and user preferences e.g. desired building temperatures. A similar concept can also be found in [1]. However, this work also focuses on incorporating and modeling essential additional aspects of the building heating, such as the building incident irradiation and insulation models, to increase accuracy. The contributions of this work can be summarized as follows:

1) A flexible HP power consumption and building temperature estimator, which can be easily re-modified according to building and heat pump model characteristics, is developed. The estimator is fed with very few accessible data inputs (weather data, HP output capacity curve, building geography, and the occupancy profile) without the use of heating demand data, which can be valuable for distribution grid studies.

2) A risk-averse "pessimistic" power-consumption HP profile is generated for grid impact and cost-saving estimation purposes. Parts of this risk-averse nature of the work are the avoidance of any buffers or thermal optimal control schemes, such as heat storage, the utilization of heat pump output capacity, and the focus on desired building temperature maintenance, during building occupation.

3) Finally, the power savings induced by the energy label enhancement of future buildings are estimated, revealing the insulation importance

This work is categorized as follows: Section III integrates the explanation of the developed power consumption concept and its submodels, Section IV contains the simulation results for 2 study cases, while discussion of the results and conclusions are presented in Sections V & VI, respectively.

III. Model of the HP Power Consumption & Temperature Simulator Concept

The total model is divided into the building, space-heating (SH), domestic hot water (DHW), insulation, and power consumption models.

A. Building Model

The building type considered in this work is the typical Dutch Terraced building, representing more than 50% of Dutch buildings. The building geography, materials, dimensions & material conductivities are presented in Table I [9], [10].

TABLE I
BUILDING PARAMETERS

Surface (surf)	Material	Area A (m^2)	Thickness d (m)	Conductivity U (W/mK)
Floor (fl)	Wood	90	0.03	0.18
Front/Back Walls (fw/bw)	Brick	15x5	0.23	1
Side Walls (sw)	Brick	6x8	0.23	1
Roof (rf)	Clay	15x4.25	0.015	0.72

$$V_b = A_{fl}H_{fw} + A_{fl}\frac{H_{fw} - H_{sw}}{2} \quad (1)$$

$$A_b = \sum_{surf\ in\ surfaces} (A_{surf}) \quad (2)$$

where roof area A_{rf} is considered twice.

Equation (1) dictates the volume of the building V_b, which is simulated as a single-zone area, according to the building geometry, where A & H represent the area & height and fl, rf, fw & sw the floor, roof, front, and side walls, respectively. Moreover, (2) shows the total building area perpendicular to the heat flow A_b, where the roof area is considered twice due to the fact that the investigated building is a terraced type.

B. Space Heating Model

The considered heat-pump layout integrates space heating and DHW heating. Due to the risk-averse nature of the work, no type of optimal control has been utilized. Therefore, a buffer tank has been used only for DHW and not for SH. For the same reason, ON-OFF air-sourced heat pumps (ASHPs) have been studied in this work, which are typically characterized by higher power consumption. The HP specifications regarding the heating & cooling output and the related water flow rates and temperatures are based on the Dimplex LIK 8MER reversible HP module [11]. The space-heating model and the concept of the simulator (Subsection H) are inspired by [1] & [7]. The built HP generation profile utilizes a timestep Δt of 1 min. While this timestep is not appropriate to catch heating transients and dynamics, it is adequate to give a reasonable accuracy to the power consumption results directed to grid simulation studies and analysis. The underlying model is presented below.

$$T_b(t + \Delta t) = \frac{\dot{Q}_{hp}(t) + \dot{Q}_{ir}(t) - \dot{Q}_{los}(t)}{C_b + V_b C_{air}\rho_{air}}\Delta t + T_b(t) \quad (3)$$

where:

$$\dot{Q}_{los}(t) = \dot{Q}_{cond}(t) + \dot{Q}_{vent}(t) \quad (4)$$

$$\dot{Q}_{cond}(t) = \sum_{surf}^{surfaces} (d_{surf}U_{surf}A_{surf})(T_b(t) - T_a(t)) \quad (5)$$

$$\dot{Q}_{vent}(t) = C_{air}\ \rho_{air}\ r_b(T_b(t) - T_a(t)) \quad (6)$$

$$\dot{Q}_{ir}(t) = G_{inc}(t)\ w_b\ s_b \quad (7)$$

Equation (3) dictates the temperature of the building T_b at every timestep Δt, which depends on the total gains of the building (HP output $\dot{Q}_{hp}$ & heat from incident solar irradiation $\dot{Q}_{ir}$), the total building losses $\dot{Q}_{los}$ (conductive losses $\dot{Q}_{cond}$ & ventilation losses $\dot{Q}_{vent}$). Moreover, it depends on the total heating capacity: the building capacity $C_b = 4.755\ kWh/K$ (a typical building value has been derived by [12]), and the capacity of the air volume inside the building, equal to $V_b = 585\ m^3$, where C_{air} and ρ_{air} represent the air's specific heat capacity and density, respectively.

The conductive & ventilation losses and incident irradiation heat gains are modeled in (5)-(7) [3], respectively, where A_{surf}, d_{surf} & U_{surf} the area, thickness & conductivity of every surface, T_b & T_a the building and ambient temperatures, r_b the air change rate of the building assumed $0.35h^{-1}$, G_{inc} the incident irradiation on the building, $w_b = 0.3$ the building's wall-to-window ratio and $s_b = 0.2$ the solar heat gain coefficient of the windows. s_b represents the heat proportion entering the building windows, considering the heat transfer by both conductivity and emissivity. It must be noted that only the solar heat transferred through the windows is taken into account, whereas the solar heat transferred through the building's walls has been ignored due to the advanced energy label of the future buildings (see Section III.F). The heat generation by house electric appliances and the people inside the buildings has also been ignored.

C. Space Cooling (SC) Model

The space cooling model resembles the space heating model. The two important differences are the utilization of the HP cooling output instead of the HP heating output and the integration of the cooling output $\dot{Q}_{hp}$ in (3) as negative.

D. Domestic Hot Water (DHW) Tank Heating

Apart from the presented space-heating & cooling models, this work also considers a DHW model, which is essential to the generated consumption profiles. DHW is highly responsible for power peaks since it is characterized by lower Coefficients of Performance (COPs) and cannot be ignored.

In this work, DHW is assumed to be realized twice daily for the residential sector, once in the morning at 06:00 a.m. and once in the evening at 19:00, and once per day for the commercial sector at 10:00 a.m. The DHW system integrates a DHW tank, which is used to heat and store hot water. Moreover, it must be noted that the HP cannot simultaneously heat space and water. Therefore, DHW is given priority at these specific time intervals of the day.

$$V_{tank} = 65(N^{0.7})125\% = \pi R_{tank}^2 H_{tank} \quad (8)$$

$$A_{tank} = 2\pi R_{tank}H_{tank} + 2\pi R_{tank}^2 \quad (9)$$

The geometry of the tank (total tank volume V_{tank} & tank area A_{tank}) is dictated by (8) & (9), according to which the tank volume depends on the number N of the people inside the building [6]. Additionally, the tank is assumed to be cylindrically shaped. R_{tank} & H_{tank} represent the tank's radius and height, respectively.

$$T_{tank}(t + \Delta t) = \frac{\dot{Q}_{hp}(t) - \dot{Q}_{los}(t)}{V_{tank} \ C_{wat} \ \rho_{wat}} \Delta t + T_{tank}(t) \quad (10)$$

$$\dot{Q}_{loss}(t) = U_{tank} A_{tank}(T_{tank}(t) - T_a(t)) \quad (11)$$

Similar to the space-heating model, the temperature of the water tank T_{tank} at every timestep Δt is calculated based on the heat gains (HP output $\dot{Q}_{hp}$), conductive losses $\dot{Q}_{loss}$ and stored water capacity. The DHW temperature and the conductive losses are dictated by (10) & (11), where C_{wat} & ρ_{wat} the water specific heat capacity and density, respectively and $U_{tank} = 0.598W/m^2K$ the tank conductivity.

E. Solar Irradiation

The total incident irradiation on the building is the sum of the incident irradiation on the four walls and the two roof surfaces. The walls are simulated as surfaces with tilt angle 90°& orientations 0°, 90°, 180°, 270° facing North, East, South & West, respectively. The two roof surfaces are simulated as two surfaces with 45° tilt angle and 0°& 180°orientation.

$$G_{inc}(t) = G_{dir}(t) + G_{dif}(t) + G_{alb}(t) \quad (12)$$

$$G_{dir}(t) = i_{DNI}(t)cos(a_i(t))A_{surf}, \ where: \quad (13)$$

$$G_{dif}(t) = i_{DHI}(t)\frac{1 + cos(\theta_{surf})}{2}A_{surf} \quad (14)$$

$$G_{alb}(t) = i_{GHI}(t)c_{alb}(1 - \frac{1 + cos(\theta_{surf})}{2})A_{surf} \quad (15)$$

$$cos(a_i(t)) = sin(\theta_{surf})cos(\theta_s(t))cos(O_{surf} - O_s(t)) + cos(\theta_{surf})sin(\theta_s(t)) \quad (16)$$

For every surface, the incident irradiation is dictated by (12) - (16). Equation (12) dictates that the total incident irradiation G_{inc} at every time moment integrates the direct irradiation G_{dir}, diffuse irradiation G_{diff} & albedo irradiation G_{alb}. The 3 types of irradiation are modeled by (13)-(15) respectively, where a_i the angle of solar incidence, c_{alb} the albedo coefficient and i_{DNI}, i_{DHI} & i_{GHI} the direct normal, diffuse horizontal & global horizontal irradiances, respectively, expressed in W/m^2. The albedo coefficient represents the proportion of irradiance reflected by the surrounding environment and has been assumed to be an average of 0.175 for the concrete sidewalks and asphalt (0.225 & 0.125, respectively). Equation (16) models the a_i, where θ_{surf} & O_{surf} the title angle and orientation (azimuth) of the surface and $\theta_s(t)$ & $O_s(t)$ the momentary solar elevation angle and orientation. It must be noted that the "Isotropic Sky Model" has been utilized for the calculation of diffuse irradiation, and potential shading by other buildings has been neglected.

F. Insulation

Another objective of this work is the revelation of the importance of enhanced building energy labels and consequently potential power savings.

$$U'_{walls} < 0.3 \ W/m^2K$$
$$U'_{roofs} < 0.18 \ W/m^2K \quad (17)$$
$$U'_{floors} < 0.22 \ W/m^2K$$

$$U_{des} = \frac{1}{\frac{d_{surf}}{U'_{surf}} + \frac{d_{ins}}{U'_{ins}}} \quad (18)$$

In (17), the European insulation norms about the conductivities of new buildings can be seen, which are greatly lower than the related ones of the typical Dutch terraced building in Table I [1]. Therefore, (17) has been utilized to insulate the building walls and roof in order to comply with the new energy label norms. According to (18), the desired conductivity U_{des} can be achieved by adding insulation material with appropriate thickness d_{ins} and conductivity U'_{ins} to the material's surface of thickness d_{mat} and conductivity U'_{mat}. It must be noted that the use of intonation to conductivity (U' or U) depends on the encapsulation of thickness d or not, respectively. The following insulation materials have been utilized:

- 80mm Expanded Polystyrene (EPS) of $U = 0.024W/mK$: Improved Walls' Conductivity U' 0.28W/m^2K
- 110mm PIR Board (Celotex) of $U = 0.019W/mK$: Improved Roof's Conductivity U' 0.17W/m^2K

G. Power Consumption Model

$$P_{hp}(t) = \frac{\dot{Q}_{hp}(t)}{COP(t)} \quad (19)$$

The HP power consumption is calculated by the well-known (19), which dictates the relation of the HP output with the COP [8].

$$COP(t) = 7.90471e^{-0.024(T_{ret}(t) - T_a(t))} \quad (20)$$

$$\dot{Q}_{hp}(t) = \dot{m}_{wat}C_{wat}(T_{sup} - T_{ret}(t))$$
$$\leftrightarrow T_{ret}(t) = T_{sup} - \frac{\dot{Q}_{hp}(t)}{\dot{m}_{wat}C_{wat}} \quad (21)$$

The utilized COP is estimated by regression from 10 different HP models [1] and is modeled in (20), where T_{ret} is the return water temperature. The return water temperature T_{ret} is calculated with the use of (21), where:

- $\dot{m}_{wat}$: flow water rate $0.8m^3/h$ both for heating and cooling operation
- T_{sup} the supply water temperature of:
    35° for floor-heating
    50° for DHW
    18° for floor-cooling [11]

[1]https://www.firstinarchitecture.co.uk/a-quick-and-easy-guide-to-u-values/

H. Power Consumption & Temperature Estimation Concept

In the last subsection, the concept of the Simulator is explained. The data inputs needed for the function of the simulator are summarized below:

- Residential & Commercial Buildings Occupancy profiles: Residential buildings are occupied throughout the day except during 08:00-14:00 on weekdays, while commercial buildings are occupied during 08:00-21:00 on weekdays and 09:00-18:00 on weekends.
- Weather data: Wind Speed w_s, Ambient Temperature T_a, Direct Normal Irradiance (i_{DNI}), Diffuse Horizontal Irradiance (i_{DHI}) & Global Horizontal Irradiance (i_{GHI}), solar elevation θ_s & solar orientation O_s. The data is downloaded by the Meteonorm database and represents average measurements for the last ten years.
- Building specifications: Materials, dimensions, parameters, and desired building temperatures (in this work always assumed 21° to 23°).
- Heat Pump Specifications: HP heating and cooling outputs with the respective space-heating, DHW-heating, and space-cooling water flow rates & temperatures.
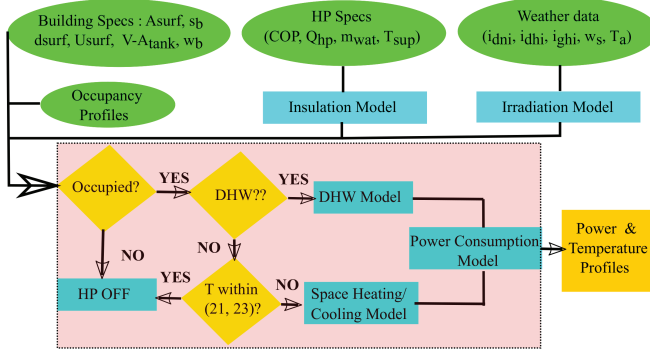

Fig. 1. Concept of HP Power Consumption Simulator

The concept of the simulator is depicted in Fig. 1. Every time instant, the algorithm is fed by the input datasets, and the momentary incident irradiation is calculated. If the building is occupied, the HP is turned ON whenever the building temperature deviates from the desired temperature interval (21°-23°). Therefore no thermal discomfort has been considered, and hence, the power consumption estimation is characterized as risk-averse. When the water tank needs to be heated (twice per day), the DHW is given priority. In any other case, the HP is turned OFF.

The next timestep's building or water tank temperatures are estimated by initially calculating the heat gains and losses by the space-heating and DHW models, respectively. From the HP output, the momentary return water temperature and COP are calculated in the Power Consumption model. Finally, the HP power consumption profile is generated.

IV. SIMULATION RESULTS

A. With compliance to new energy label norms

In this subsection, the insulation model is considered, and the HP operation in heating and cooling mode is depicted during a winter and a summer week, respectively. In this regard, the diurnal and seasonal effects on the HP operation, COP levels & power consumption are captured.
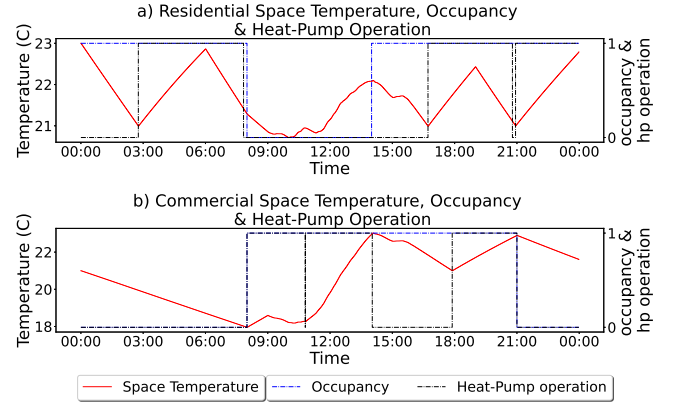

Fig. 2. Daily Winter Residential (a) & Commercial (b) Space Temperature, Occupancy & HP ON-OFF Operation

1) Winter Heating Period: In Fig. 2, the building temperature, as well as the occupancy profile and the HP ON-OFF operation, can be seen for the residential (Fig. 2a) and the commercial buildings (Fig. 2b) for a period of a day. As it can be observed, the HP is always turned off when the buildings are not occupied, while it is always turned on at the occupation time instant if the temperature is below 21°. Moreover, as soon as the temperature enters the desired interval, it always stays between 21 & 23°. The space-heating & DHW COPs are
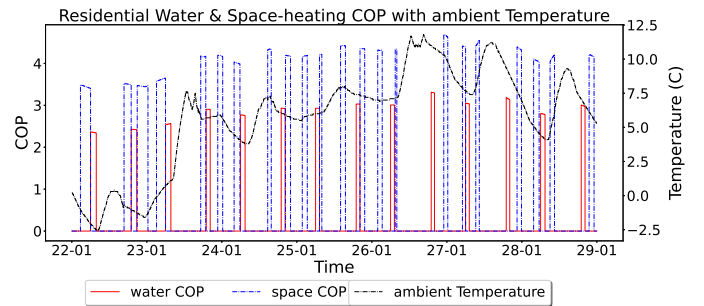

Fig. 3. Winter Residential SH/DHW COPs & ambient Temperature

plotted with the ambient Temperature for the whole winter week in Fig. 3. The space-heating COPs fluctuate between 3.4 and 4.4, while the DHW COP fluctuates between 2.3 and 3.3. The increased space-heating COP has been expected, due to the higher heating temperature of the DHW, compared with the floor-heating temperature. Moreover, a relative increase of both COPs is observed with the increase in the ambient Temperature. The consequences of the lower DHW COPS on
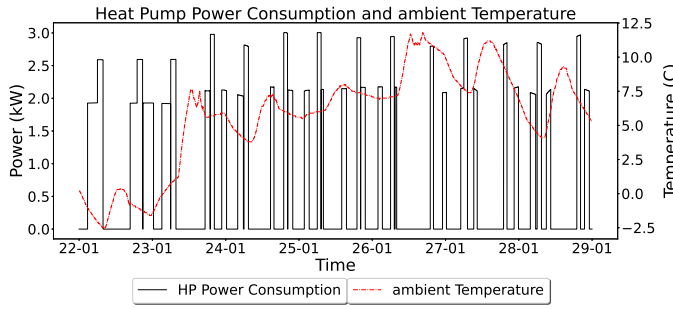
Fig. 4. Winter Residential Consumption & ambient Temperature

the HP power consumption can be seen in Fig. 4. While the HP consumption for space-heating deviates mostly around 2kWs, it can reach up to 3kWs, when the DHW operation is on. However, the HP Power Consumption fluctuates less than the COP during variable ambient Temperatures. This is due to the fact that both the COP and the heating capacity increase during higher ambient temperatures, both of which affect the HP power consumption.
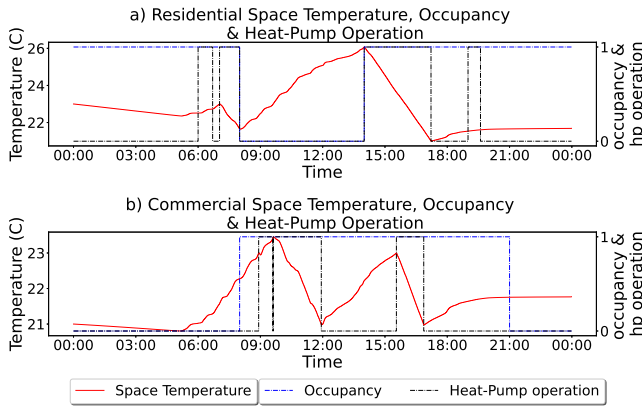

Fig. 5. Daily Summer a) Residential & b) Commercial Space Temperature, Occupancy & HP ON-OFF Operation
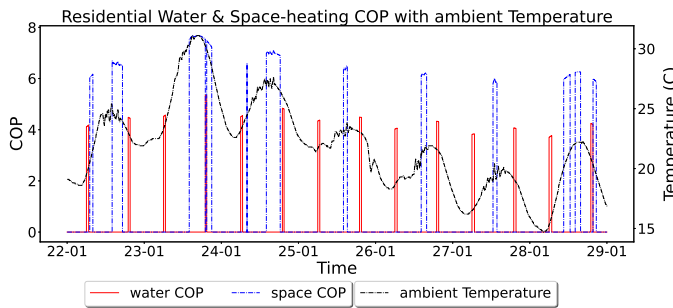

Fig. 6. Summer Residential SC-DHW COPs and ambient Temperature

2) Summer Cooling Period: In Fig. 5a, the residential building temperature exceeds 23°and reaches up to 26° only when the building is not occupied, while similar results can be observed for the commercial buildings in Fig. 5b. Figs. 6-7
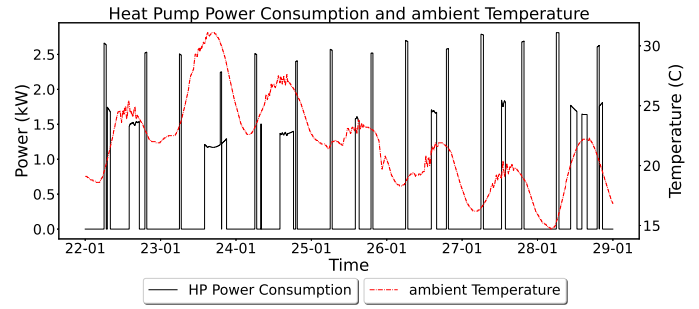

Fig. 7. Summer Residential Consumption & ambient Temperature

present the space-cooling & DHW COPs as well as the power consumption with the ambient temperature for the summer week period, respectively. During this period, the DHW is heated with COPs deviating between 4 and 5.1, while the space-cooling is performed with COPs between 6 and 7.8. In this regard, the high peaks of the HP power consumption, which fluctuate between 2.3kWs and 2.7kWs, belong to the DHW operation, while the low peaks (between 1.2kWs and 1.7kWs) represent the space-cooling operation.

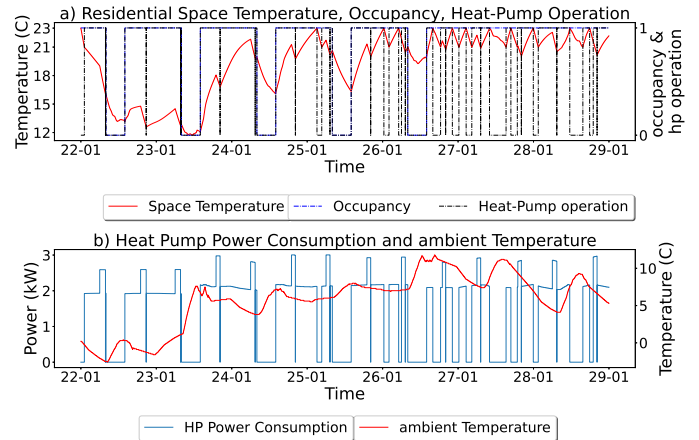*B. Without compliance to new energy label norms*

Fig. 8. Weekly Residential Non-insulated Building Temperature (a) & Power Consumption (b) versus ambient Temperature

Here the irradiation model is not considered to reveal the importance of the new energy norms and insulation for future buildings that are heated by HPs. In Fig. 8, the residential building temperature with the HP ON-OFF operation (a) & the power consumption with the ambient temperature (b) are depicted for the winter period. As it can be observed, the ON operation intervals of the HP last much longer, compared to Fig. 4 (reaching up to even 150% higher ON durations) than in the insulated buildings, leading to higher consumption. Moreover, we can see that for the first three days of the week, which are characterized by very low ambient temperatures, the HP fails to keep the building temperature within the desired thermal comfort, due to the higher losses. An HP with a

higher power rating and heat capacity would be needed for the particular non-insulated building.
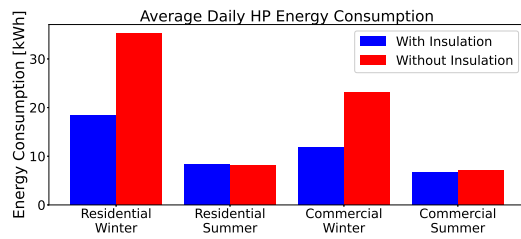

Fig. 9. Daily Average HP Energy Consumption with & without Insulation

Fig. 9 visualizes the difference of the HP energy consumption in non-insulated and insulated buildings for the four investigated study cases (residential & commercial sectors during winter & summer). While during the summer period, the variation of the results can be considered negligible, the power consumption is highly increased during winter, rising to a daily average of 35kWhs and 24kWhs from 18kWhs and 12kWhs for residential and commercial buildings, respectively. Hence, a daily average 94% & 100% consumption increase is observed for the residential and commercial buildings.

V. Discussion

In section V, the most important outcomes of the results section of this work are summarized. Initially, the effects of DHW and space heating/cooling on the HP operation COPs have been shown. The DHW operation is characterized by highly decreased COPs of an average percentage of 29% and 34% during winter and summer, respectively.

Moreover, the summer period is more favorable for space heating/cooling operations and power consumption. Space cooling is performed with an average COP of 6.9, which is approximately 77% increased compared with the average space-heating COP of 3.9. Furthermore, an 80% increase in the DHW operation COP is observed during summer, while the power consumption is decreased up to 1.3kW compared to the high consumption peaks during winter (around 2.5kWs and 3kWs for space-heating and DHW, respectively). One of the main reasons for this behavior is the more moderate summer ambient temperatures that characterize the Netherlands. While the winter ambient Temperature drops even below 0°, the summer ambient temperature fluctuates mostly between 20°and 30°, which is close to the desired thermal comfort.

Finally, the significant importance of the new insulation norms for future buildings is also revealed in this work. The daily average power consumption is double when the building is not insulated, while we have also seen that the same HP module has failed to keep the building temperature for the first half of the week in the second case.

VI. Conclusion

In this work, an HP power consumption and building temperature estimator has been developed with the advantage of limited needed data since it does not need the availability of heating demand data. Therefore, it can be easily modified according to different building and HP parameters. Moreover, the risk-averse character of power consumption estimation (no optimal control, no thermal discomfort, use of HP output capacity) can be proven valuable for grid impact and cost-saving studies, protecting against uncertainty. The COP and power consumption behaviors have been analyzed during different seasons, while the importance of insulation has been also revealed (nearly double power consumption). This work did not consider uncertainty, such as different building parameters, HP models, or occupancy profiles, which are recommended as future work of this simulator. Additionally, the impact of electric heaters on power consumption, usually provided with HPs for backup, should also be investigated.

References

[1] R. O. Oliyide and L. M. Cipcigan, "The impacts of electric vehicles and heat pumps load profiles on low voltage distribution networks in great britain by 2050," in *International Multidisciplinary Research Journal*, vol. 11, 2021, pp. 30–45.

[2] B. Asare-Bediako, W. Kling, and P. Ribeiro, "Future residential load profiles: Scenario-based analysis of high penetration of heavy loads and distributed generation," *Energy and Buildings*, vol. 75, pp. 228–238, 2014. [Online]. Available: https://www.sciencedirect.com/science/article/pii/S037877881400139X

[3] B. Abhinandana, K. Beddiar, Y. Amirat, and M. Benbouzid, "Simplified building thermal model development and parameters evaluation using a stochastic approach," *Energies*, vol. 13, pp. 1–23, 06 2020.

[4] S. M. Rahman, "Simplified 3r2c building thermal network model: A case study," 07 2019.

[5] M. Koroli and O. Ishnazarov, "Mathematical modeling of a heat pump and its operation modes," *E3S Web of Conferences*, vol. 216, p. 01165, 01 2020.

[6] D. Fischer, K. B. Lindberg, H. Madani, and C. Wittwer, "Impact of pv and variable prices on optimal system sizing for heat pumps and thermal storage," *Energy and Buildings*, vol. 128, pp. 723–733, 2016. [Online]. Available: https://www.sciencedirect.com/science/article/pii/S037877881630603X

[7] L. Ferrarini, S. Rastegarpour, and L. Caseri, "Predictive control-oriented models of a domestic air-to-water heat pump under variable conditions," *IEEE Robotics and Automation Letters*, vol. 5, no. 4, pp. 5363–5369, 2020.

[8] T. Terlouw, T. AlSkaif, C. Bauer, and W. van Sark, "Optimal energy management in all-electric residential energy systems with heat and electricity storage," *Applied Energy*, vol. 254, p. 113580, 2019. [Online]. Available: https://www.sciencedirect.com/science/article/pii/S0306261919312541

[9] R. Esposito, F. Messali, G. Ravenshorst, R. Schipper, and J. Rots, "Seismic assessment of a lab-tested two-storey unreinforced masonry dutch terraced house," *Bulletin of Earthquake Engineering*, vol. 17, 08 2019.

[10] T. Awadallah, H. Adas, Y. Obaidat, and I. Jarrar, "Energy efficient building code for jordan," 01 2009.

[11] Dimplex. Project planning manual heating and cooling with heat pumps. Dimplex. [Online]. Available: https://www.dimplex-partner.de/fileadmin/dimplex/downloads/planungshandbuecher/en

[12] S. A. Tabatabaei, W. Van der Ham, M. C. A. Klein, and J. Treur, "A data analysis technique to estimate the thermal characteristics of a house," *Energies*, vol. 10, no. 9, 2017. [Online]. Available: https://www.mdpi.com/1996-1073/10/9/1358